Inorganic Chemistry

Article

pubs.acs.org/IC

Metal-Induced Isomerization of a Molecular Strand Containing Contradictory Dynamic Coordination Sites

Daniel J. Hutchinson, Matthew P. James, Lyall R. Hanton,* and Stephen C. Moratti

Department of Chemistry, University of Otago, P.O. Box 56, Dunedin, New Zealand

Supporting Information

ABSTRACT: A new hydroxymethyl terminated pyrimidine-hydrazone (pym-hyz) ligand (**L1**) was synthesized with a central hyz-pyridine-hyz (hyz-py-hyz) motif replacing the usual hyz-pym-hyz unit, to create a molecular strand that underwent metal-induced isomerization with a minimal net change in ligand length. NMR spectroscopy showed that **L1** had a horseshoe shape due to the hyz-py-hyz and pym-hyz bonds adopting transoid conformations. The ligand was successfully reacted with Pb(II), Zn(II), and Ag(I) salts in either CH_3CN or CH_3NO_2 resulting in horseshoe-shaped $M^{n+}{}_3\mathbf{L1}A_{3n}$ (where A = ClO_4^- or $SO_3CF_3^-$) complexes in the solution phase. Crystals were grown from these solutions, the structures of which were highly dependent on the metal ion and solvent used, and were distinctly different from those seen in solution. The crystals grown from mixtures of $Pb(ClO_4)_2{\cdot}3H_2O$ and **L1** in either CH_3CN or CH_3NO_2 resulted in the horseshoe-shaped $[Pb_3\mathbf{L1}(ClO_4)_4(H_2O)_2](ClO_4)_2{\cdot}CH_3CN$ (**1**) complex or the $\{[Pb_3\mathbf{L1}(ClO_4)_4(H_2O)](ClO_4)_2\}_\infty{\cdot}CH_3NO_2$ (**2**) helical coordination polymer, respectively. The horseshoe-shaped $[Pb_3\mathbf{L1}(SO_3CF_3)_6]{\cdot}CH_3CN$ (**3**) complex was crystallized from a solution of $Pb(SO_3CF_3)_2{\cdot}H_2O$ and **L1** in CH_3CN, while the crystals grown from the solution of $Zn(SO_3CF_3)_2$ and **L1** in CH_3CN consisted of the zigzag-shaped $[Zn_3\mathbf{L1}(H_2O)_7](SO_3CF_3)_6$ (**4**) complex. The $[Ag_3(\mathbf{L1})_2](SO_3CF_3)_3$ (**5**) double-helicate and the macrocycle-like $[Ag_6(\mathbf{L1})_2](SO_3CF_3)_6$ (**6**) complex were crystallized from solutions of $AgSO_3CF_3$ and **L1** in either CH_3CN or CH_3NO_2, respectively.

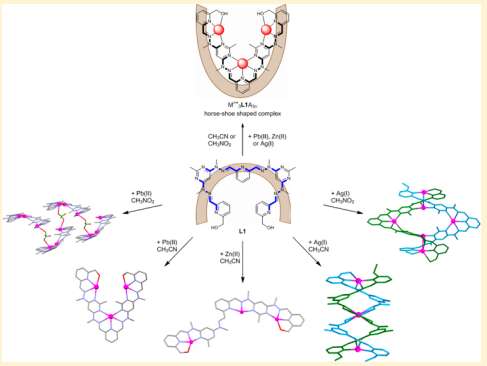

INTRODUCTION

The pyrimidine-hydrazone (pym-hyz) unit acts as a dynamic helicity codon by enforcing helicity on a molecular strand and by isomerizing into a linearity codon upon coordinating metal ions.[1] This isomerization is driven by the rotation of the transoid pym-hyz bonds to a cisoid conformation to form a tridentate coordination site.[2] As a result, molecular strands of repeating pym-hyz strands have been shown to undergo significant, and reversible, one-dimensional extensions upon their reaction with suitable metal ions.[1,3]

Our research aims to harness the significant conformational change exhibited by pym-hyz molecular strands for use in powering polymer gel-based actuators.[4] Such gels have emerged as actuating technologies in the realms of robotics and microfludics[5] due to their ability to absorb solvent and swell in size upon the application of an external stimulus.[6] It is our hypothesis that the extent of swelling expressed by the pym-hyz containing polymer gels would be dependent on the amplitude of extension exhibited by the pym-hyz ligands upon the addition of metal ions. Thus far, we have synthesized pym-hyz strands consisting of three[7,8] and five[9] aromatic rings, which undergo changes in length of approximately 7 and 24 Å, respectively, upon reacting them with metal salts of Pb(II), Zn(II), and Cu(II) ions. These ligands contain terminal hydroxymethyl functional groups, which, when treated with acryloyl chloride, are converted into acryloyl functional groups,[4,10] allowing for the incorporation of the pym-hyz ligands into covalent polymer networks by radical polymerization.[11]

Efforts to synthesize longer pym-hyz strands with terminal hydroxymethyl arms are ongoing; however, it would also be advantageous to design a pym-hyz strand that underwent metal-induced isomerization but did not exhibit a significant extension in length. If the expansion of the pym-hyz gels was dependent on the amplitude of ligand extension, then the gel containing this ligand would not be expected to swell in size upon absorbing metal ions. This gel could therefore be treated as a negative control when investigating the correlation between the extension amplitude of the pym-hyz ligands and the magnitude of swelling displayed by their gels. The pym-hyz ligand **L1** has been designed specifically for this purpose. The ligand contains two terminal pym-hyz-py coordination sites joined by a central hyz-py-hyz unit. This central unit is isostructural to a py-py-py motif, which has been previously shown to have a linear transoid−transoid conformation that rotates to a bent cisoid−cisoid conformation upon metal ion coordination (Figure 1).[12] Therefore, the pym-hyz-py and hyz-py-hyz coordination sites of **L1** isomerize due to metal ion coordination in a contradictory fashion. Consequently, **L1** was expected to undergo significant localized isomerization while displaying a smaller overall

Received: October 31, 2013
Published: February 5, 2014

   dx.doi.org/10.1021/ic4027392 | *Inorg. Chem.* 2014, 53, 2122−2132

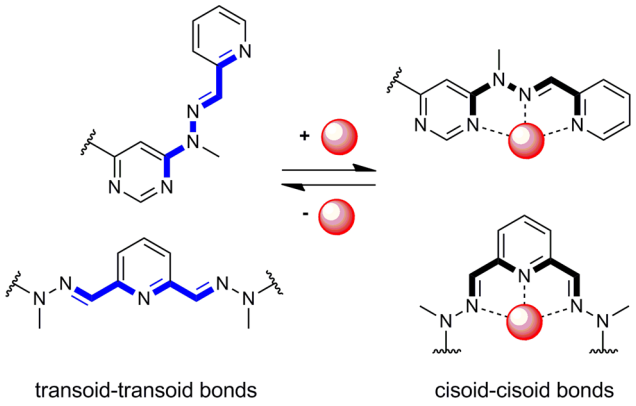

Figure 1. The conformational changes of the pym-hyz-py (top) and hyz-py-hyz (bottom) units upon the coordination of a metal ion (red). The transoid bonds are highlighted in blue, whereas the cisoid bonds are highlighted in black.

amplitude of extension than that of the previously synthesized pym-hyz molecular strands.

L1 was successfully synthesized and reacted with salts of Pb(II), Zn(II), and Ag(I) ions in an attempt to characterize the behavior of the contradictory hyz-py-hyz and pym-hyz-py coordination sites. The addition of metal ions resulted in the rotation of the pym-hyz and py-hyz linkages from their energetically favored transoid conformations[1,13] to cisoid conformations, resulting in $M^{n+}{}_3\mathbf{L1}A_{3n}$ (where A = ClO_4^- or $SO_3CF_3^-$) complexes that had an overall structure that was similar to that of **L1**. Crystals were grown from the CH_3CN and CH_3NO_2 solutions of the metal salts and **L1** which displayed a variety of structures that were affected by the choice of solvent and metal ion. The results showed that the contradictory behavior of the coordination sites in **L1** gave the ligand a highly flexible nature which allowed for the synthesis of discrete complexes, coordination polymers, double helicates, and macrocycle-like dimers (Figure 2).

EXPERIMENTAL SECTION

General. All starting materials, reagents, and metal salts were purchased from commercial sources and were used as received without further purification, with the exception of $Pb(SO_3CF_3)_2{\cdot}H_2O$ which was produced through the treatment of $2PbCO_3{\cdot}Pb(OH)_2$ with aqueous triflic acid. 6-Hydroxymethyl-2-pyridinecarboxaldehyde, 2-methyl-2-[6-(1-methylhydrazinyl)-4-pyrimidinyl]hydrazine (**AB**) was synthesized from the precursors 4,6-bis(1-methylhydrazino)-2-methylpyrimidine (**A**)[14] and 6-hydroxymethyl-2-pyridinecarboxaldehyde (**B**)[15] as described in the literature.[9] 2,6-Pyrimidinedicarboxaldehyde

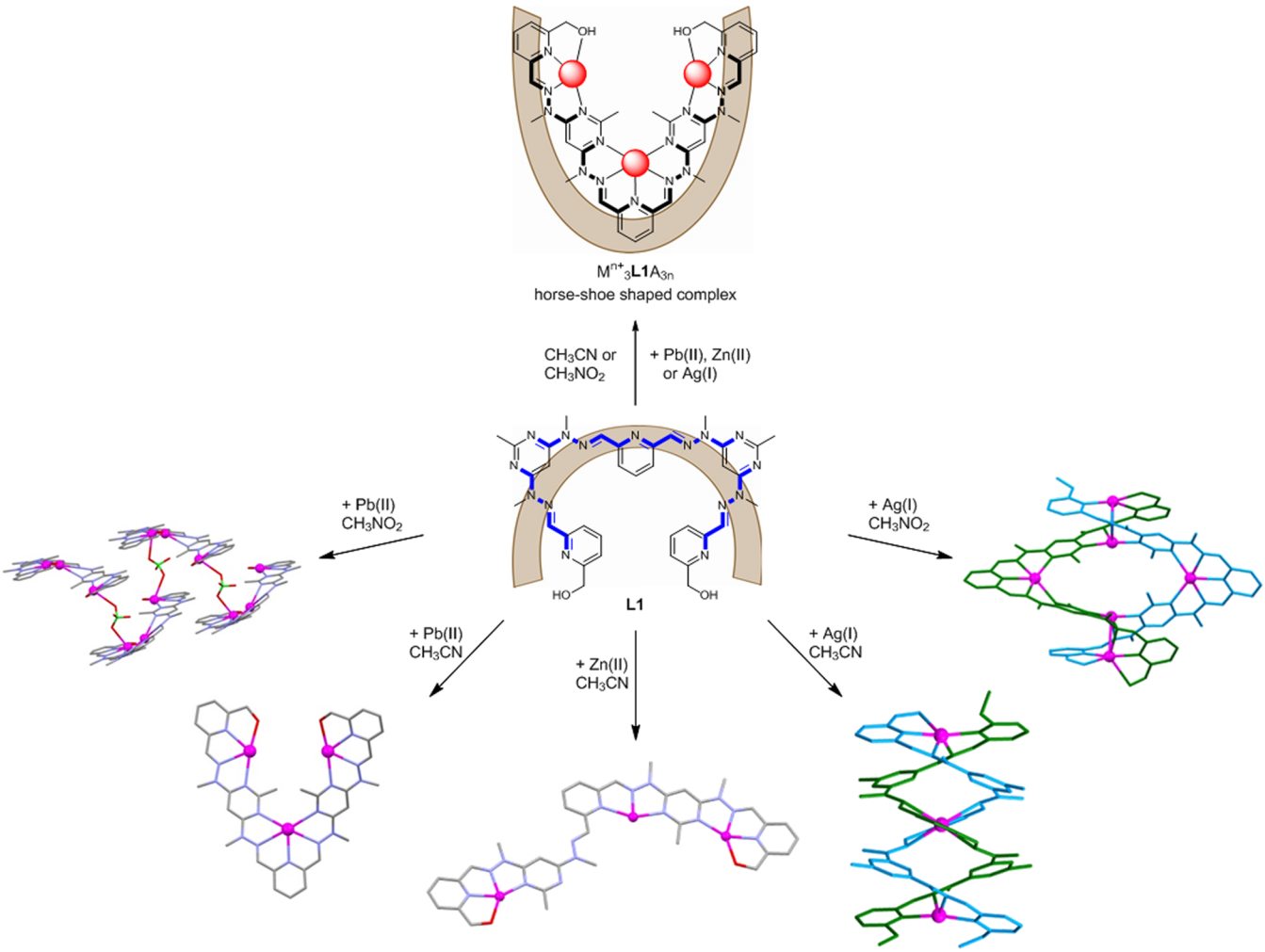

Figure 2. The addition of Pb(II), Zn(II), or Ag(I) ions to **L1** resulted in horseshoe-shaped complexes in the solution phase (top) and a variety of complex structures depending on the choice of solvent and metal ion in the solid state (bottom).

dx.doi.org/10.1021/ic4027392 | Inorg. Chem. 2014, 53, 2122−2132

(**C**) was collected as a byproduct during the purification of **B**. All solvents were used as received and were LR grade or better.

Microanalyses were carried out in the Campbell Microanalytical Laboratory, University of Otago. All measured microanalysis results had an uncertainty of ±0.4%. ^{1}H and ^{13}C NMR spectra and two-dimensional (gCOSY, NOSEY, HSQC, gHMBC, DOSY) spectra were collected on a 500 MHz Varian UNITY INOVA spectrometer at 298 K. Spectra were collected in either CD_3CN or CD_3NO_2 or a mixture of CD_3CN and CF_3SO_3D (1:10 v/v) and were referenced to the internal solvent signal, with chemical shifts reported in δ units (ppm). Electrospray mass spectrometry (ESMS) was carried out on a Bruker microTOFQ instrument (Bruker Daltronics, Bremen, Germany) by employing direct infusion into an ESI source in positive mode. Infrared (IR) spectra were recorded on a Bruker Alpha-P ATR-IR spectrometer.

Synthesis of Ligand L1. **AB** (1.07 g, 3.57 mmol) and **C** (0.206 g, 1.52 mmol) were refluxed in EtOH (100 mL) for 4 h, resulting in the precipitation of a white solid. The reaction mixture was filtered, and the white precipitate was washed with EtOH and dried in vacuo: **L1** (1.03 g, 96%). Anal. Found. C 58.72; H 5.58; N 29.22. Calc. for $C_{35}H_{39}N_{15}O_2{\cdot}H_2O$: C 58.40; H 5.74; N 29.19. ^{1}H NMR (500 MHz, CD_3CN/SO_3CF_3D 10:1 v/v) δ/ppm: 8.65 (1H, t, J = 8.0 Hz, H4), 8.61 (2H, t, J = 8.0 Hz, H18), 8.53 (2H, d, J = 8.0 Hz, H3/5), 8.49 (2H, s, H7), 8.35 (2H, s, H15), 8.26 (2H, d, J = 7.8 Hz, H17), 8.01 (2H, d, J = 8.0 Hz, H19), 7.43 (2H, s, H10), 5.11 (4H, s, H21), 3.82 (6H, s H14), 3.81 (6H, s, H8), 2.83 (6H, s, H13). ^{13}C NMR (500 MHz, CD_3CN/SO_3CF_3D 10:1 *v/v*) δ/ppm: 162.9 (C12), 158.5 (C20), 148.5 (C18), 147.6 (C4), 147.4 (C2/6), 144.9 (C16), 135.7 (C7), 135.0 (C15), 127.3 (C3/5), 126.6 (C17), 126.0 (C19), 87.8 (C10), 60.5 (C21), 33.3 (C14), 33.2 (C8), 22.8 (C13). ESMS m/z Found: 702.3537, 351.6821. Calc. for $C_{35}H_{40}N_{15}O_2^{+}$: 702.3484. Calc. for $C_{35}H_{41}N_{15}O_2^{2+}$: 351.6779. Selected IR ν/cm^{-1}: 3354 (m, br), 3251 (m, br, OH str), 2917 (m, CH str), 1590 (s), 1559 (s, C═N str), 1484 (s), 1450 (s), 1432 (m), 1410 (m), 1394 (s), 1263 (m), 1236 (m), 1215 (s), 1166 (s), 1043 (s).

Synthesis of Pb_3L1$(ClO_4)_6$. A solution of $Pb(ClO_4)_2{\cdot}3H_2O$ (78.4 mg, 0.193 mmol) in CH_3CN (5.00 mL) was added to **L1** (34.4 mg, 0.0490 mmol) and stirred at 70 °C for 1 h, resulting in the dissolution of **L1** and the formation of a bright yellow solution. The addition of diethyl ether (20.0 mL) resulted in the precipitation of a yellow solid, which was filtered and washed with diethyl ether before being dried in vacuo (39.6 mmol, 42%): Anal. Found: C 21.49; H 2.46; N 10.93. Calc for $C_{35}H_{39}N_{15}O_{27}Cl_6Pb_3{\cdot}3H_2O$: C 21.49; H 2.22; N 10.74. ^{1}H NMR (500 MHz, CD_3CN) δ/ppm: 8.74 (2H, s, H15), 8.66 (2H, s, H7), 8.36 (1H, t, J = 7.8 Hz, H4), 8.20 (2H, t, J = 7.8 Hz, H18), 8.04 (2H, d, J = 7.8 Hz, H3/5), 7.95 (2H, d, J = 7.5 Hz, H17), 7.68 (2H, d, J = 7.9 Hz, H19), 6.65 (2H, s, H10), 5.95 (2H, s, br, H22), 5.30 (4H, s, H21), 3.77 (6H, s, H14), 3.76 (6H, s, H8), 2.74 (6H, s, H13). ^{13}C NMR (500 MHz, CD_3CN) δ/ppm: 167.5 (C12), 162.2 (C20), 161.7 (C9), 161.2 (C11), 152.3 (C2/6), 150.3 (C16), 144.1 (C15), 143.4 (C7), 142.9 (C4), 142.0 (C18), 129.9 (C3/5), 128.1 (C17), 125.2 (C19), 87.4 (C10), 65.6 (C21), 35.9 (C14), 35.7 (C8), 26.6 (C13). ESMS m/z Found: 1820.0083. Calc. for $C_{35}H_{39}N_{15}O_2Pb_3(ClO_4)_5^{+}$: 1820.0091. Selected IR ν/cm^{-1}: 3403 (w, br, OH str), 3080 (w, CH str), 2978 (w, CH str), 1585 (m), 1537 (s, C═N str), 1484 (m), 1451 (m), 1432 (m), 1403 (m), 1386 (m), 1366 (w), 1292 (m), 1260 (m), 1158 (m), 1081 (s, ClO_4^{-}), 1019 (s, br). Crystals suitable for X-ray diffraction were grown by the slow diffusion of diethyl ether into CH_3CN or CH_3NO_2 solutions of $Pb(ClO_4)_2{\cdot}3H_2O$ and **L1** in a 4:1 ratio. These crystals gave the structures $[Pb_3$**L1**$(ClO_4)_4(H_2O)_2]$-$(ClO_4)_2{\cdot}CH_3CN$ (**1**) and $\{[Pb_3$**L1**$(ClO_4)_4(H_2O)](ClO_4)_2\}_\infty{\cdot}$ CH_3NO_2 (**2**), respectively.

Synthesis of Pb_3L1$(SO_3CF_3)_6$. As described for Pb_3**L1**$(ClO_4)_6$ but with $Pb(SO_3CF_3)_2{.}H_2O$ (117 mg, 0.223 mmol), **L1** (38.9 mg, 0.0555 mmol) stirring in CH_3CN (5.00 mL); yellow solid (60.6 mg, 49%): Anal. Found: C 22.15; H 2.13; N 9.02. Calc. for $C_{41}H_{39}N_{15}O_{20}F_{18}S_6Pb_3{\cdot}H_2O$: C 22.03; H 1.85; N 9.40. ^{1}H NMR (500 MHz, CD_3CN) δ/ppm: 8.71 (2H, s, H15), 8.63 (2H, s, H7), 8.37 (1H, t, J = 7.8 Hz, H4), 8.21 (2H, t, J = 7.7 Hz, H18), 8.02 (2H, d, J = 7.8 Hz, H3/5), 7.93 (2H, d, J = 7.5 Hz, H17), 7.68 (2H, d, J = 7.9 Hz, H19), 6.65 (2H, s, H10), 5.88 (2H, br, H22), 5.31 (4H, s, H21), 3.75 (12H, s, H8/14), 2.74 (6H, s, H13). ESMS m/z Found: 724.3169, 702.3361. Calc. for $C_{35}H_{39}N_{15}O_2Na^{+}$: 724.3309. Calc. for $C_{35}H_{40}N_{15}O_2^{+}$: 702.3489. Selected IR ν/cm^{-1}: 3334 (w, br, OH str), 1585 (m), 1551 (s, C═N str), 1537 (s), 1487 (m), 1454 (m), 1434 (m), 1389 (m), 1367 (w), 1217 (s, $SO_3CF_3^{-}$), 1154 (s), 1047 (s), 1018 (s). Crystals suitable for X-ray diffraction were grown by the slow diffusion of diethyl ether into a CH_3CN solution of $Pb(SO_3CF_3)_2{\cdot}H_2O$ and **L1** in a 4:1 ratio. These crystals gave the structure $[Pb_3$**L1**$(SO_3CF_3)_6]{\cdot}CH_3CN$ (**3**).

Synthesis of Zn_3L1$(SO_3CF_3)_6$. As described for Pb_3**L1**$(ClO_4)_6$ but with $Zn(SO_3CF_3)_2$ (60.8 mg, 0.167 mmol) **L1** (38.6 mg, 0.0551 mmol) stirring in CH_3CN (5.00 mL); yellow solid (48.6 mg, 49%): Anal. Found: C 26.50; H 2.90; N 10.90. Calc. for $C_{41}H_{39}N_{15}O_{20}F_{18}S_6Zn_3{\cdot}5H_2O$: C 26.16; H 2.62; N 11.16. ^{1}H NMR (500 MHz, CD_3CN) δ/ppm: 8.42 (2H, br, H7), 8.33 (1H, t, J = 7.8 Hz, H4), 8.30 (2H, br, H15), 8.19 (2H, t, J = 7.8 Hz, H18), 7.83 (2H, d, J = 7.4 Hz, H17), 7.62 (2H, d, J = 8.0 Hz, H19), 7.05 (2H, br, H10), 6.66 (2H, t, J = 3.6 Hz, H22), 5.08 (4H, d, J = 3.7 Hz, H21), 3.85 (6H, s, H8), 3.78 (6H, s, H14), 2.90 (6H, br, H13). ^{13}C NMR (500 MHz, CD_3CN) δ/ppm: 167.2 (br, C12), 158.9 (C11), 157.9 (C20), 148.6 (C2/6), 146.4 (C16), 143.2 (C18), 143.1 (C4), 138.4 (C9), 136.0 (br, C15), 131.9 (C7), 125.4 (br, C17), 124.5 (br, C19), 86.5 (C10), 61.6 (C21), 34.1 (C8/14), 26.8 (C13). ESMS m/z Found: 764.2573, 414.5899, 382.6352. Calc. for $C_{35}H_{38}N_{15}O_2Zn^{+}$: 764.2619. Calc. for $C_{35}H_{37}N_{15}O_2Zn_2^{2+}$: 414.5898. Calc. for $C_{35}H_{39}N_{15}O_2Zn^{2+}$: 382.6346. Selected IR ν/cm^{-1}: 3338 (w, br, OH str), 1631 (w), 1598 (m), 1569 (m), 1551 (m, C═N str), 1448 (m), 1449 (m), 1436 (m), 1421 (m), 1391 (w), 1366 (w), 1271 (m), 1233 (s), 1220 (s, $SO_3CF_3^{-}$), 1156 (s), 1121 (m), 1053 (m), 1023 (s). Crystals suitable for X-ray diffraction were grown by the slow diffusion of diethyl ether into a CH_3CN solution of $Zn(SO_3CF_3)_2$ and **L1** in a 3:1 ratio These crystals gave the structure $[Zn_3$**L1**$(H_2O)_7](SO_3CF_3)_6$ (**4**).

Synthesis of Ag_3L1$(SO_3CF_3)_3$ in CH_3CN. As described for Pb_3**L1**$(ClO_4)_6$ but with $AgSO_3CF_3$ (40.2 mg, 0.157 mmol) and **L1** (35.0 mg, 0.0499 mmol) stirring in CH_3CN (5.00 mL); yellow solid (45.5 mg, 62%): Anal. Found: C 32.14; H 3.12; N 15.06. Calc. for $C_{38}H_{39}N_{15}O_{11}F_9S_3Ag_3{\cdot}CH_3CN$: C 32.45; H 2.92; N 15.32. ^{1}H NMR (500 MHz, CD_3CN) δ/ppm: 7.93 (1H, t, J = 7.8 Hz, H4), 7.88 (2H, t, J = 7.7 Hz, H18), 7.74 (2H, s, H15), 7.48 (2H, d, J = 7.7 Hz, H17), 7.30 (2H, dd, J = 1.0, 8.0 Hz, H3/5), 7.21 (2H, d, J = 7.8 Hz, H19), 7.11 (2H, s, H7), 6.84 (2H, s, H10), 3.84 (2H, dd, J = 5.3, 14.8 Hz, H21a), 3.76 (2H, dd, J = 5.7, 14.8 Hz, H21b), 3.47 (2H, t, J = 5.5 Hz, H22), 3.13 (6H, s, H14), 2.94 (6H, s, H14), 2.31 (6H, s, H13). ^{13}C NMR (500 MHz, CD_3CN) δ/ppm: 166.7 (C12), 162.5 (C9/11), 161.6 (C20), 151.1 (C2/6), 150.5 (C16), 140.5 (C18), 140.4 (C4), 139.0 (C15), 136.4 (C7), 126.3 (C3/5), 125.5 (C17), 123.8 (C19), 89.9 (C10), 64.9 (C21), 32.29 (C14), 31.7 (C8), 26.0 (C13). Selected IR ν/cm^{-1}: 3401 (w, br, OH str), 3080 (w, CH str), 2902 (w, CH str), 1574 (s), 1541 (s, C═N str), 1479 (s), 1457 (m), 1406 (s), 1246 (s, $SO_3CF_3^{-}$), 1223 (s), 1154 (s), 1090 (m), 1042 (s). ESMS m/z Found: 1066.1012, 808.2457, 458.5743. Calc. for $C_{35}H_{39}N_{15}O_2Ag_2(SO_3CF_3)^{+}$: 1066.1025. Calc. for $C_{35}H_{39}N_{15}O_2Ag^{+}$: 808.2457. Calc. for $C_{35}H_{39}N_{15}O_2Ag_2^{2+}$: 458.5750. Crystals suitable for X-ray diffraction were grown by the slow diffusion of diethyl ether into a CH_3CN solution of $AgSO_3CF_3$ and **L1** in a 4:1 ratio. These crystals gave the structure $[Ag_3(\mathbf{L1})_2](SO_3CF_3)_3$ (**5**).

Synthesis of Ag_3L1$(SO_3CF_3)_3$ in CH_3NO_2. As described for Pb_3**L1**$(ClO_4)_6$ but with $AgSO_3CF_3$ (48.2 mg, 0.188 mmol) and **L1** (43.6 mg, 0.0622 mmol) stirring in CH_3NO_2 (5.00 mL) at 100 °C; brown solid (24.7 mg, 27%): Anal. Found: C 30.72; H 2.72; N 14.16. Calc. for $C_{38}H_{39}N_{15}O_{11}F_9S_3Ag_3$: C 30.99; H 2.67; N 14.27. ^{1}H NMR (500 MHz, CD_3NO_2) δ/ppm: 8.52 (1H, s, $H15_A$), 8.41 (1H, s, $H7_A$), 8.32 (1H, s, $H15_B$), 8.21 ($H7_B$), 8.11 (1H, t, J = 7.8 Hz, $H18_A$), 8.06 (1H, t, J = 7.8 Hz, $H18_B$), 8.01 (1H, t, J = 7.8 Hz, H4), 7.81 (1H, d, J = 7.7 Hz, $H17_A$), 7.78 (1H, m, H3), 7.76 (1H, m, $H17_B$), 7.56 (1H, d, J = 7.6 Hz, H5), 7.30 (1H, d, J = 7.8 Hz, $H19_A$), 7.27 (1H, d, J = 7.7 Hz, $H19_B$), 6.99 (1H, s, $H10_B$), 6.75 (1H, s, $H10_A$), 4.43 (1H, d, J = 15.4 Hz, $H21_A$), 4.29 (1H, d, J = 16.1 Hz, $H21_B$), 3.86 (3H, s, $H8_B$), 3.85 (3H, s, $H8_A$), 3.75 (3H, s, $H14_A$), 3.61 (3H, s, $H14_B$), 3.31 (1H, d, J =

dx.doi.org/10.1021/ic4027392 | Inorg. Chem. 2014, 53, 2122−2132

Table 1. Crystallographic Data for the Complexes of L1

	$[Pb_3\mathbf{L1}(ClO_4)_4(H_2O)_2]\ (ClO_4)_2{\cdot}CH_3CN$ (**1**)	$\{[Pb_3\mathbf{L1}(ClO_4)_4(H_2O)]\ (ClO_4)_2\}_\infty{\cdot}CH_3NO_2$ (**2**)	$[Pb_3\mathbf{L1}(SO_3CF_3)_6]{\cdot}CH_3CN$ (**3**)
formula	$C_{37}H_{42}Cl_6N_{16}O_{28}Pb_3$	$C_{36}H_{42}Cl_6N_{16}O_{29}Pb_3$	$C_{43}H_{42}F_{18}N_{16}O_{20}Pb_3S_6$
formula weight	1993.14	1997.13	2258.95
crystal system	triclinic	monoclinic	triclinic
space group	$P\bar{1}$	$P2_1/n$	$P\bar{1}$
a/Å	9.9128(10)	22.3152(3)	14.3516(9)
b/Å	14.6570(16)	11.64703(16)	15.9545(9)
c/Å	25.946(3)	25.6567(4)	17.4788(11)
α/°	93.371(4)	90	103.245(2)
β/°	92.665(4)	103.2066(14)	92.541(3)
γ/°	103.775(4)	90	102.890(2)
V/Å^3	3647.9(7)	6491.95(16)	3778.3(4)
Z	2	4	2
T/K	90(2)	100(2)	90(2)
μ/mm^{-1}	7.206	17.831	6.950
reflections collected	43560	101608	42897
unique reflections (R_{int})	13436 (0.0588)	12072 (0.1221)	14038 (0.0480)
R_1 indices [$I > 2\sigma(I)$]	0.0513	0.0933	0.0472
wR_2 (all data)	0.1427	0.2330	0.1328
goodness of fit	1.105	1.036	1.019
	$[Zn_3\mathbf{L1}(H_2O)_7](SO_3CF_3)_6$ (**4**)	$[Ag_3(\mathbf{L1})_2](SO_3CF_3)_3$ (**5**)	$[Ag_6(\mathbf{L1})_2](SO_3CF_3)_6$ (**6**)
formula	$C_{38}H_{43}F_9N_{15}O_{18}S_3Zn_3$	$C_{72}H_{78}Ag_3F_6N_{30}O_{10}S_2$	$C_{72}H_{77}Ag_6F_6N_{30}O_{10}S_2$
formula weight	1461.16	2025.40	2348.00
crystal system	monoclinic	monoclinic	monoclinic
space group	$P2_1/n$	$P2_1/n$	$I2/a$
a/Å	23.791(4)	15.9060(4)	34.0737(14)
b/Å	8.4896(16)	20.1642(6)	20.2018(13)
c/Å	40.356(7)	28.7161(12)	33.1437(11)
α/°	90	90	90
β/°	103.753(6)	98.747(3)	91.233(3)
γ/°	90	90	90
V/Å^3	7918(4)	9103.0(5)	22809(2)
Z	4	4	8
T/K	90(2)	100(2)	100(2)
μ/mm^{-1}	1.060	0.766	9.010
reflections collected	36052	74844	63787
unique reflections (R_{int})	13956 (0.0523)	16929 (0.0616)	21059 (0.0577)
R_1 indices [$I > 2\sigma(I)$]	0.0763	0.0957	0.0901
wR_2 (all data)	0.2117	0.2472	0.2857
goodness of fit	1.070	1.079	0.998

15.3 Hz, H21$_A$), 3.24 (1H, d, J = 15.5 Hz, H21$_B$), 2.52 (3H, s, H13$_B$), 2.32 (3H, s, H13$_A$). ^{13}C NMR (500 MHz, CD_3NO_2) δ/ppm: 167.1 (C12$_A$), 166.5 (C12$_B$), 164.0 (C9$_B$), 161.1 (C11$_B$), 160.2 (C11$_A$), 159.8 (C9$_A$), 159.7 (C20$_B$), 159.6 (C20$_A$), 150.5 (C6), 150.4 (C16$_B$), 150.3 (C16$_A$), 149.0 (C2), 143.3 (C7$_A$), 143.2 (C15$_A$), 140.6 (C4), 140.3 (C15$_B$), 139.9 (C18$_A$), 139.7 (C18$_B$), 138.4 (C7$_B$), 128.3 (C3), 127.6 (C5), 126.3 (C17$_A$), 126.0 (C17$_B$), 124.21 (C19$_A$), 123.7 (C19$_B$), 91.4 (C10$_B$), 89.41 (C10$_A$), 61.6 (C21$_B$), 61.4 (C21$_A$), 35.6 (C14$_B$), 35.5 (C8$_A$), 34.5 (C14$_A$), 32.2 (C8$_B$), 31.45 (C13$_A$), 27.69 (C13$_B$). ESMS m/z Found: 808.2398, 458.5713. Calc. for $C_{35}H_{39}N_{15}O_2Ag^+$: 808.2457. Calc. for $C_{35}H_{39}N_{15}O_2Ag_2^{2+}$: 458.5750. Selected ν/cm^{-1}: 3391 (w, br, OH str), 3082 (w, CH str), 2927 (w, CH str), 1577 (m), 1538 (s, C═N str), 1482 (m), 1452 (m), 1429 (m), 1403 (m), 1383 (m), 1271 (s), 1241 (s, $SO_3CF_3^-$), 1221 (s), 1150 (s), 1042 (s), 1023 (s). Crystals suitable for X-ray diffraction were grown by the slow diffusion of diethyl ether into a CH_3NO_2 solution of $AgSO_3CF_3$ and **L1** in a 7:1 ratio. These crystals gave the structure $[Ag_6(\mathbf{L1})_2](SO_3CF_3)_6$ (**6**).

X-ray Crystallography. Crystallographic data are summarized in Table 1. Thermal ellipsoid pictures of complexes **1**−**6** and selected bond lengths and angles are available in the Supporting Information, along with a description of how the disordered components of the complexes were treated. The X-ray diffraction data for complexes **1**, **3**, and **4** were collected on a Bruker APEX II CCD diffractometer, with graphite monochromated Mo Kα (λ = 0.71073 Å) radiation. Intensities were corrected for Lorentz polarization effects[16] and a multiscan absorption correction[17] was applied. The X-ray diffraction data for complexes **2**, **5**, and **6** were collected on an Agilent Supernova dual radiation source XRD with an Atlas detector. The radiation source used was either mirror monochromated Mo for complex **5** or Cu (λ = 1.5418 Å) for complexes **2** and **6**. The data for complexes **2**, **5**, and **6** were processed using Agilent CrysAlisPro software (version 1.171.36),[18] which was also used to apply either multiscan (complex **2**) or Gaussian (complexes **5** and **6**) absorption corrections.

The structures for complexes **1**−**6** were solved by direct methods (SHELXS[19] or SIR-97[20]) and refined on F^2 using all data by full-matrix least-squares procedures (SHELXL 97[21]). All calculations were performed using the WinGX interface.[22] Detailed analyses of the extended structure were carried out using PLATON[23] and MERCURY[24] (Version 2.4).

RESULTS AND DISCUSSION

Synthesis and Structure of L1. Ligand **L1** was formed through a double condensation reaction between the building

dx.doi.org/10.1021/ic4027392 | Inorg. Chem. 2014, 53, 2122−2132

Scheme 1. Synthesis of L1 from the Reaction of AB and C in a 2:1 Molar Ratio in EtOH[a]

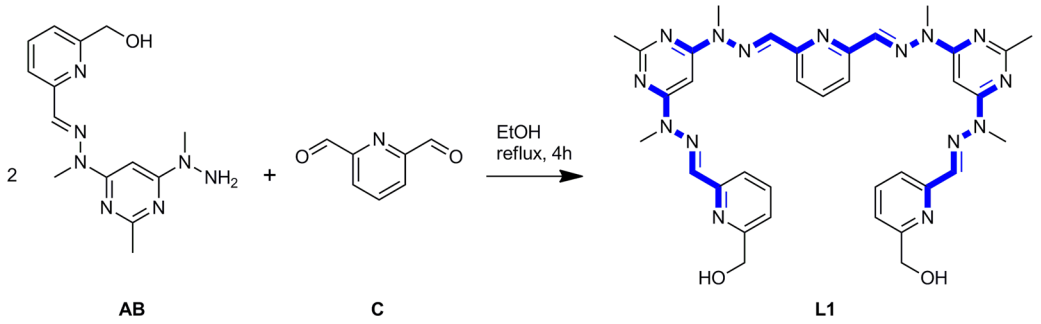

[a]The transoid bonds of **L1** are highlighted blue.

blocks 6-hydroxymethyl-2-pyridinecarboxaldehyde, 2-methyl-2-[6-(1-methylhydrazinyl)-4-pyrimidinyl]hydrazine (**AB**) and 2,6-pyrimidinedicarboxaldehyde (**C**) in a 2:1 molar ratio. Performing the reaction in EtOH under refluxing conditions resulted in the precipitation of **L1** as a pure white solid in a very high yield of between 90 and 96% (Scheme 1).

The ESMS spectrum of **L1** showed peaks corresponding to the $[\mathbf{L1} + H]^+$ and $[\mathbf{L1} + 2H]^{2+}$ molecular ions, while the IR spectrum showed a strong peak at 1559 cm^{-1} due to the C═N stretching mode, a broad O−H stretching mode at 3251 cm^{-1}, and multiple peaks representing the pyridine (py) and pyrimidine (pym) rings and hydrazone (hyz) linkages. The low solubility of **L1** in all commonly used organic solvents made probing its structure by NMR spectroscopy difficult. Eventually, it was discovered that **L1** could be solubilized in CD_3CN through protonation by the addition of a minimal volume of SO_3CF_3D (1:10 v/v), which resulted in a yellow solution. NOE correlations showed that the protonated form of **L1** contained a mixture of transoid and cisoid pym-hyz and py-hyz bonds (Figure 3). However, these bonds were assumed to

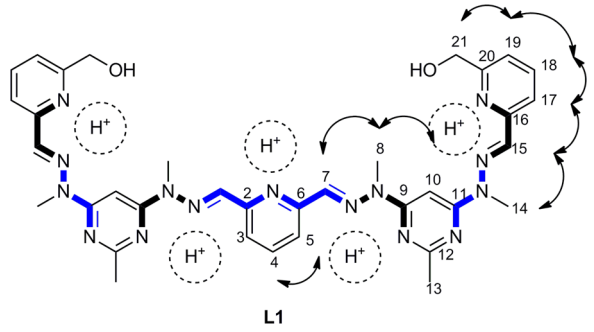

Figure 3. Structure of the protonated form of **L1**, which contained a mixture of transoid (blue) and cisoid (black) pym-hyz and py-hyz linkages, as indicated by NOE correlations (protons were placed by assuming that, under the experimental conditions, each heterocycle was monoprotonated).

adopt their energetically favored transoid conformations in the unprotonated form of **L1** due to (i) the significant energy difference of 20−30 kJ mol^{-1} between the transoid and cisoid conformations of bipyridine,[13] of which the pym-hyz and py-hyz bonds are isomorphic,[2] (ii) the insistence of the pym-hyz and py-hyz bonds of **L1** to adopt transoid conformations when not coordinated to metal ions in complexes **4** and **5** (Figures 5, 9, and 11), (iii) the prevalence of transoid pym-hyz and py-hyz bonds in a pym-hyz-py macrocycle described in the literature,[25] and finally (iv) the conformation of the hydroxymethyl terminated ditopic pym-hyz ligand previously described by our group which contains transoid pym-hyz and py-hyz linkages.[8] Upon dissolving this ditopic ligand in CD_3CN with the aid of SO_3CF_3D, it too was protonated and displayed cisoid pym-hyz and py-hyz linkages. Despite the change in shape of **L1** caused by protonation, many of the signals in its ^1H and ^{13}C NMR spectra were similar to those of other native and unprotonated pym-hyz ligands.[1,8,9] The H10 signal of the protonated form of **L1** was located at 7.43 ppm, which was typical of pym protons adjacent to transoid pym-hyz linkages, despite H10 being between one transoid and one cisoid pym-hyz linkage. The chemical shifts of the hyz imine protons and the terminal py protons were also similar to those of uncoordinated pym-hyz ligands. Unfortunately, crystals of **L1** could not be grown for X-ray diffraction, despite numerous attempts with both slow evaporation and diethyl ether vapor diffusion methods.

Synthesis and Structures of Complexes. The treatment of **L1** with metal salts such as $Pb(ClO_4)_2{\cdot}3H_2O$, $Pb(SO_3CF_3)_2{\cdot}H_2O$, $Zn(SO_3CF_3)_2$, and $AgSO_3CF_3$ resulted in dissolution of the ligand material to form yellow solutions, with heating and stirring, in either CH_3CN or CH_3NO_2. Complete dissolution of **L1** required that at least a 3:1 metal to ligand ratio be used. The addition of diethyl ether to these solutions resulted in yellow precipitates which were analyzed by microanalysis, ESMS, and IR spectroscopy. The reactions were also repeated in either CD_3CN or CD_3NO_2 so that the composition of the solutions could be elucidated by NMR spectroscopy. Crystals of the **L1** complexes were grown by the slow addition of diethyl ether by vapor diffusion. **L1** was also reacted with $Zn(BF_4)_2$ and $AgBF_4$; however, these salts failed to solubilize **L1** at any metal to ligand ratio in either CH_3CN or CH_3NO_2.

The microanalysis results from the solids produced by reacting **L1** with the Pb(II), Zn(II) and Ag(I) salts were consistent with the composition of $M^{n+}{}_3\mathbf{L1}A_{3n}$ complexes (where A = ClO_4^- or $SO_3CF_3^-$). The ESMS spectra of the $Pb_3\mathbf{L1}(ClO_4)_6$ and $Pb_3\mathbf{L1}(SO_3CF_3)_6$ complexes showed peaks due to the $[Pb_3\mathbf{L1}(ClO_4)_5]^+$ and $[\mathbf{L1} + H]^+$ molecular ions, respectively. The $Zn_3\mathbf{L1}(SO_3CF_3)_6$ complex produced an ESMS spectrum containing peaks due to the $[Zn_2\mathbf{L1} - 2H]^{2+}$, $[Zn\mathbf{L1}]^{2+}$ and $[Zn\mathbf{L1} - H]^+$ molecular ions. The Ag(I) complexes of **L1** synthesized in CH_3CN and CH_3NO_2 produced ESMS spectra containing peaks due to the $[Ag_2\mathbf{L1}(SO_3CF_3)]^+$, $[Ag_2\mathbf{L1}]^{2+}$, and $[Ag\mathbf{L1}]^+$ molecular ions.

The IR spectra of the complexes showed that the coordination of metal ions to the **L1** ligand shifted the C═N stretching mode from 1559 cm^{-1} to between 1551 and 1537 cm^{-1}. The broad O−H stretching modes of the complexes were

dx.doi.org/10.1021/ic4027392 | Inorg. Chem. 2014, 53, 2122−2132

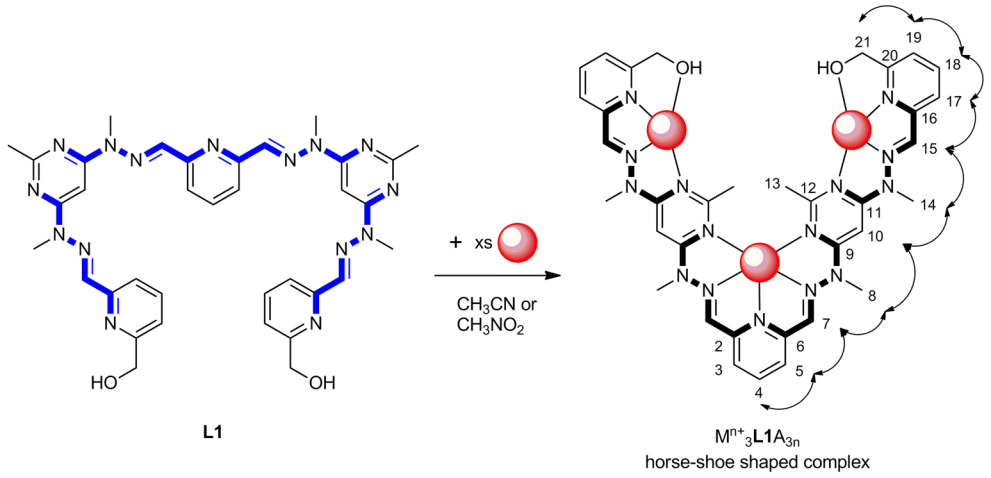

Figure 4. The conformational change of **L1** upon coordination with Pb(II), Zn(II), or Ag(I) ions in CH_3CN or CH_3NO_2 as determined by ^1H NMR spectroscopy, showing the NOE correlations which were diagnostic of the horseshoe-like shape of the $M^{n+}{}_3\mathbf{L1}A_{3n}$ complexes (NMR numbering).

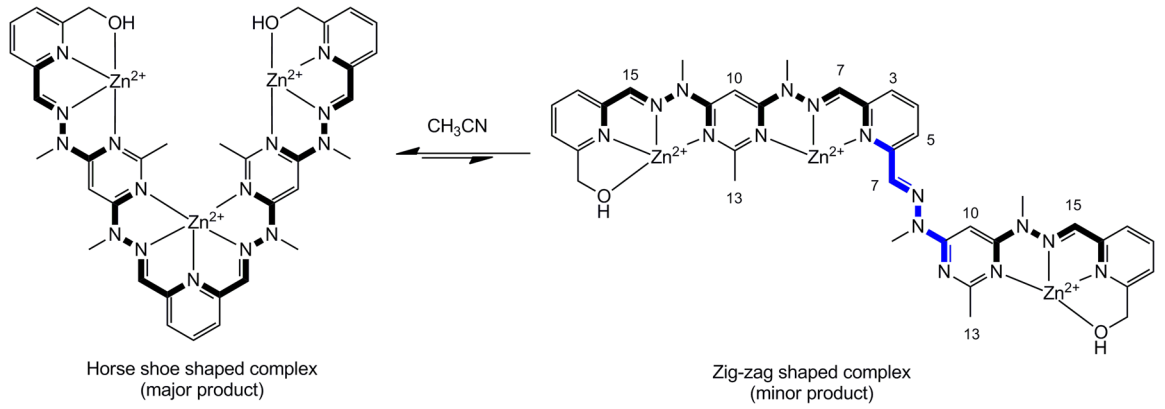

Figure 5. The structures of the two $Zn_3\mathbf{L1}(SO_3CF_3)_6$ complexes present in CD_3CN as indicated by the extensive broadening of the NMR signals for the protons labeled (NMR numbering).

located between 3403 and 3334 cm^{-1}, which were significantly higher in frequency than the O−H stretching mode of the native ligand, which was present at 3251 cm^{-1}. Each of the complexes either showed a ClO_4^- stretching mode at 1081 cm^{-1} or a $SO_3CF_3^-$ stretching mode between 1246 and 1217 cm^{-1}.

Analysis of the mixtures of **L1** and the Pb(II), Zn(II), and Ag(I) salts in either CD_3CN or CD_3NO_2 by 2D NOESY NMR spectroscopy revealed that the $M^{n+}{}_3\mathbf{L1}A_{3n}$ complexes were horseshoe-shaped, with metal ions bound to the central py-hyz-py and the terminal pym-hyz-py pockets. This resulted in the isomerization of the py-hyz-py site from a transoid−transoid conformation to a cisoid−cisoid conformation, causing a bend in the ligand backbone. The terminal pym-hyz-py coordination sites of the complexes adopted linear cisoid−cisoid conformations, as seen previously for other pym-hyz based ligands (Figure 4).[1,4,7,8]

The formation of these horseshoe-shaped $M^{n+}{}_3\mathbf{L1}A_{3n}$ complexes resulted in a number of diagnostic chemical shift changes in their ^1H NMR spectra. For example, in the ^1H NMR spectrum of each of the $Pb_3\mathbf{L1}A_6$ complexes, the H10 signal was shifted upfield from its chemical shift of 7.43 ppm in the protonated **L1** spectrum to 6.65 ppm, due to the removal of the deshielding effects from the adjacent hyz linkage upon rotation of the transoid pym-hyz bond to a cisoid conformation.[1,13] The H3/5 and H4 protons of the central py ring were also shifted upfield upon the addition of Pb(II) ions due to the rotation of the central py-hyz bonds from transoid to cisoid conformations. The withdrawal of electron density from the terminal py rings and the hyz groups by the newly coordinated Pb(II) ions resulted in deshielding of the H7, H15, H17, H18, and H19 protons.

It appeared that the $Zn_3\mathbf{L1}(SO_3CF_3)_6$ complex existed in an equilibrium between two conformations in CD_3CN. One of these conformations was the horseshoe-shaped complex, while the other was a zigzag-shaped complex, in which the Zn(II) ion bound to the central py ring was also bound to only one of the adjacent hyz functions and to the nearby pym ring (Figure 5). As a result, the central hyz-py-hyz motif had a transoid−cisoid conformation, resulting in a twist at the center of the **L1** molecule. The fluxional nature of the $Zn_3\mathbf{L1}(SO_3CF_3)_6$ complex in CD_3CN resulted in significant broadening of the H7, H10, H13, and H15 signals in the ^1H NMR spectrum. The H3/5 signals could not be distinguished from the rest of the aromatic peaks. Additionally, the slow addition of diethyl ether into the CH_3CN solution of $Zn(SO_3CF_3)_2$ and **L1** resulted in the crystallization of the zigzag-shaped complex (**4**) as opposed to the horseshoe-shaped complex.

Two different isomers of the $Ag_3\mathbf{L1}(SO_3CF_3)_3$ complex were observed in CD_3NO_2 by NMR spectroscopy, one of which was

dx.doi.org/10.1021/ic4027392 | Inorg. Chem. 2014, 53, 2122−2132

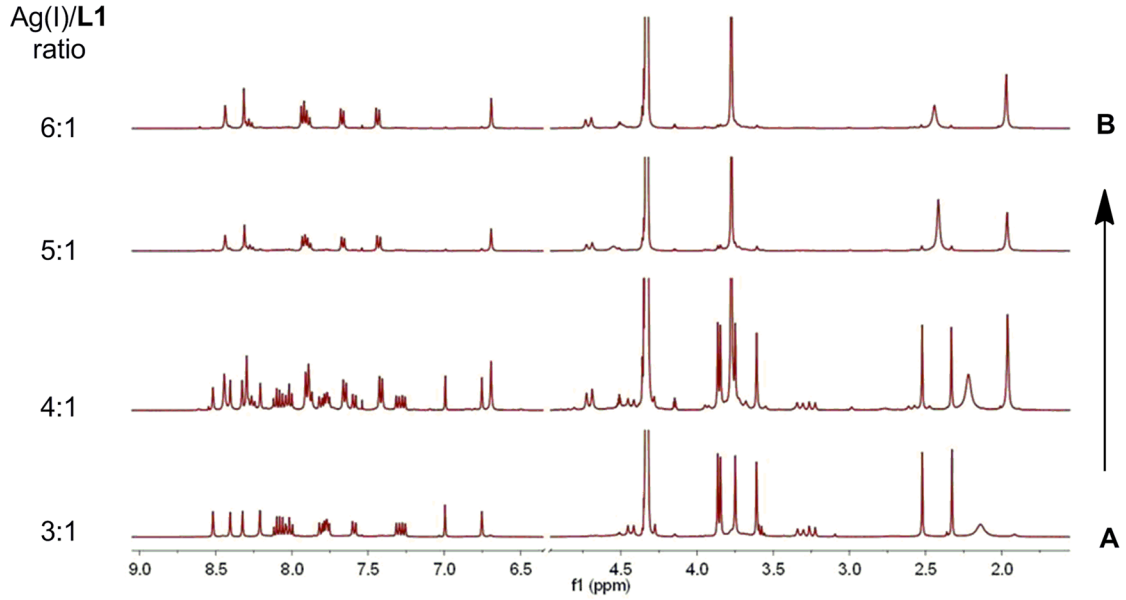

Figure 6. Increasing the Ag(I) to **L1** ratio in CD_3NO_2 from 3:1 to 6:1 resulted in a shift from the dissymmetric $Ag_3\mathbf{L1}(SO_3CF_3)_3$ isomer (**A**), to the symmetric isomer (**B**).

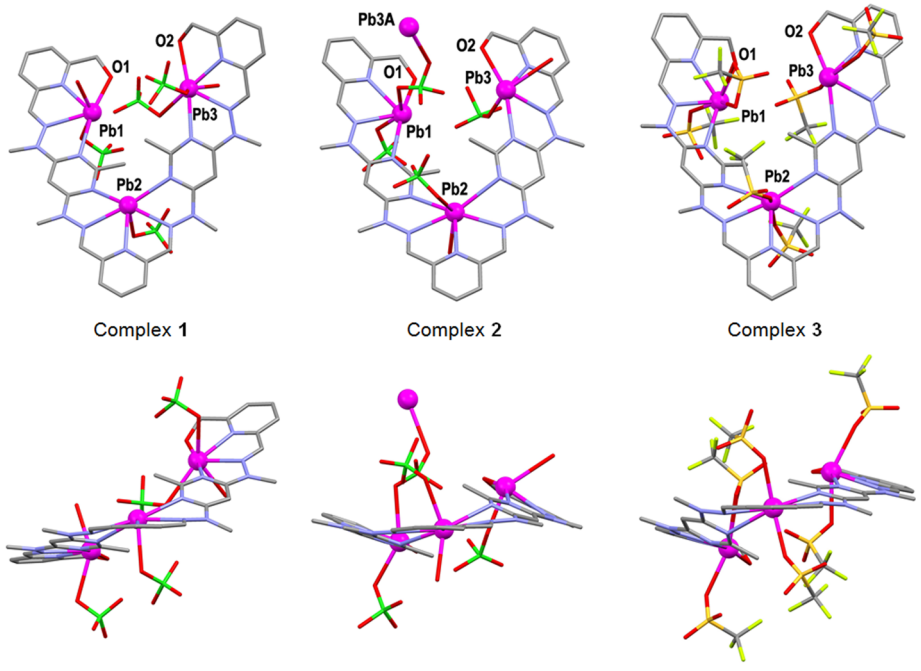

Figure 7. Views of the cations of complexes **1**−**3** showing the horseshoe shape of the complexes (top) and the complexes through the plane of the central py ring (bottom; crystallographic numbering; symmetry code A: $^3/_2 - x, -1/2 + y, 1/2 - z$).

symmetric while the other was asymmetric about the axis bisecting the central py ring. A DOSY NMR experiment was run on a mixture of the two isomers, which showed the isomers had similar diffusion coefficients. This suggested that their hydrodynamic radii, and therefore overall sizes, were similar.[26] NOE correlations showed that both isomers were horseshoe-shaped with all py-hyz and pym-hyz bonds in their cisoid conformations. It therefore appeared that the cause of asymmetry in the dissymmetric isomer was a difference in the binding geometries of the Ag(I) ions bound to the terminal pym-hyz-py binding pockets. There was a lack of NOE correlations between the methylene protons of the hydroxymethyl arms and the py rings in the dissymmetric isomer, suggesting that the hydroxymethyl arms were orientated away from the Ag(I) ions. In contrast, the NOE correlations of the symmetric complex indicated binding between the hydroxymethyl arms and the Ag(I) ions. The methylene protons of both isomers were diastereotopic, indicating that the positioning of the hydroxymethyl arms was fixed. The dissymmetric compound was present at a metal to ligand ratio of 3:1. Increasing the metal to ligand ratio resulted in its conversion to the symmetric complex (Figure 6). Only the symmetrical $Ag_3\mathbf{L1}(SO_3CF_3)_3$ isomer was observed in CD_3CN.

X-ray Crystallography. X-ray quality crystals were grown by the slow diffusion of diethyl ether into the CH_3CN or CH_3NO_2 solutions of the $M^{n+}{}_3\mathbf{L1}A_{3n}$ complexes. These crystals

dx.doi.org/10.1021/ic4027392 | Inorg. Chem. 2014, 53, 2122−2132

yielded the structures **1**–**6**. Of these structures, only the Pb_3**L1**A_6 complexes (**1**–**3**) had horseshoe-shaped conformations which were similar to those seen in solution by NMR spectroscopy. The solid state structure of the Zn_3**L1**$(SO_3CF_3)_6$ complex (**4**) had a zigzag shape, while the $AgSO_3CF_3$ complex of **L1** which crystallized from CH_3CN was a Ag_3(**L1**)$_2(SO_3CF_3)_3$ double-helicate (**5**), and the complex crystallized from CH_3NO_2 consisted of two Ag_3**L1**$(SO_3CF_3)_3$ molecules joined through coordination between the Ag(I) ions and the hydroxymethyl arms of the **L1** molecules and Ag–Ag bonds (**6**).

Complexes 1–4: Pb(II) and Zn(II) Complexes of L1. Crystals of $[Pb_3$**L1**$(ClO_4)_4(H_2O)_2]$ $(ClO_4)_2{\cdot}CH_3CN$ (**1**) and $\{[Pb_3$**L1**$(ClO_4)_4(H_2O)](ClO_4)_2\}_\infty{\cdot}CH_3NO_2$ (**2**) were grown from solutions of $Pb(ClO_4)_2$ and **L1** in either CH_3CN, or CH_3NO_2, respectively, while $[Pb_3$**L1**$(SO_3CF_3)_6]{\cdot}CH_3CN$ (**3**) was crystallized from a CH_3CN solution of $Pb(SO_3CF_3)_2$ and **L1**. Each of the Pb(II) complexes consisted of horseshoe-shaped Pb_3**L1**A_6 molecules. Pb(II) ions were bound to the three N donors and the hydroxymethyl arms of each pym-hyz-py coordination pocket and the five N donors of the central hyz-py-hyz unit. The coordination spheres of the Pb(II) ions were then completed with either ClO_4^- or $SO_3CF_3^-$ anions, H_2O molecules or stereochemically active lone pairs of electrons.[27] The solid state structures of these complexes differed from their solution phase structures, as complexes **1**–**3** were not symmetrical and were instead twisted such that the terminal py rings were located on opposite sides of the plane through the central py ring (Figure 7). The distances between the centroids of the terminal py rings for complexes **1**–**3** were 13.2, 9.8, and 10.2 Å, respectively.

While complexes **1** and **3** were discrete molecules, complex **2** existed as a helical coordination polymer running in the [0 1 0] direction due to the O21 and O24 containing ClO_4^- anion bridging adjacent complex molecules through coordination to Pb1 and Pb3 (Figure 8). With the exception of H_2O molecules, none of complexes **1**–**3** showed any coordination of solvent molecules to the Pb(II) ions; however, they all contained uncoordinated CH_3CN or CH_3NO_2 molecules in their asymmetric units.

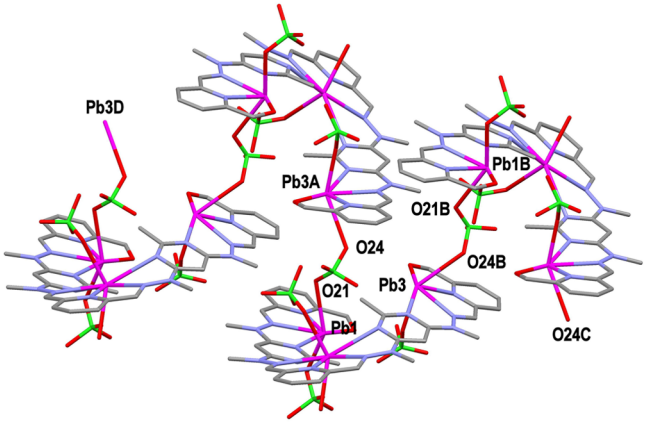

Figure 8. View of the helical coordination polymer complex **2**, formed by a ClO_4^- anion bridging Pb1 and Pb3 on adjacent complex molecules (crystallographic numbering; symmetry codes A: $^3/_2 - x$, $1/2 + y$, $1/2 - z$; B: $^3/_2 - x$, $-1/2 + y$, $1/2 - z$; C: x, $-1 + y$, z; D: x, $1 + y$, z).

While NMR spectroscopy showed that the Zn_3**L1**$(SO_3CF_3)_6$ complex had predominately a horseshoe shape in solution, the only complex that was crystallized from CH_3CN was a zigzag-shaped complex, $[Zn_3$**L1**$(H_2O)_7](SO_3CF_3)_6$ (**4**; Figure 9).

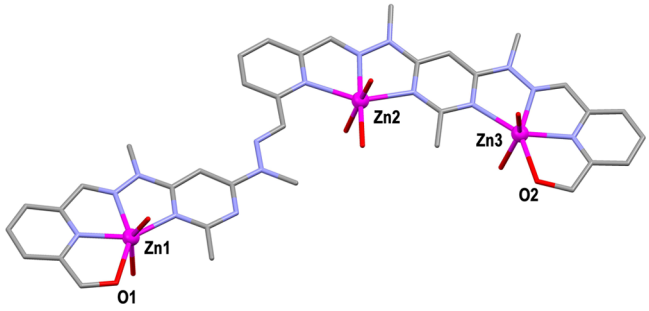

Figure 9. View of the $[Zn_3$**L1**$(H_2O)_7]^{6+}$ cation of complex **4** showing its zigzag-like shape.

Complex **4** contained a Zn(II) ion bound to the three N donors and the hydroxymethyl arms of each pym-hyz-py coordination site. The Zn(II) ion bound to the central py ring was also bound to one of the two N donors of the neighboring hyz-pym linkage. As a result, the central hyz-py-hyz unit had a transoid–cisoid conformation resulting in a twisted, or zigzag, like shape. Each of the Zn(II) ions was octahedral in geometry, with H_2O molecules completing their coordination spheres. The centroid-to-centroid distance between the terminal py rings was 23.4 Å.

Three of the six $SO_3CF_3^-$ anions were removed from the X-ray structural solution of complex **4** by use of the PLATON SQUEEZE[23] procedure due to intense disorder. The three anions that remained linked the $[Zn_3$**L1**$(H_2O)_7]^{6+}$ cations together into an infinite one-dimensional chain in the [0 1 0] direction through H-bonding with the coordinated H_2O molecules (Figure 10).

Complexes 5 and 6: Ag(I) Complexes of L1. Attempts to crystallize the horseshoe-shaped Ag_3**L1**$(SO_3CF_3)_3$ complex, which was identified in solution by NMR spectroscopy, from either CH_3CN or CH_3NO_2 resulted in crystals of either the

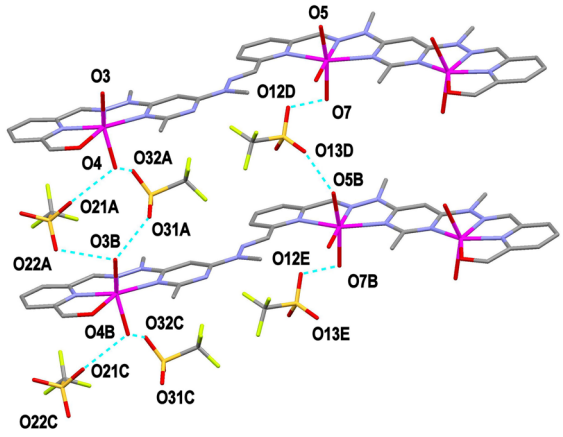

Figure 10. The association of two $[Zn_3$**L1**$(H_2O)_7]^{6+}$ cations through H-bonding interactions involving the three resolved $SO_3CF_3^-$ anions. These interactions arranged complex **4** into a one-dimensional chain in the [0 1 0] direction (symmetry codes A: $1/2 - x$, $-1/2 + y$, $^3/_2 - z$; B: x, $-1 + y$, z; C: $1/2 - x$, $-^3/_2 + y$, $^3/_2 - z$; D: x, $-1 + y$, z; E: x, $-2 + y$, z).

dx.doi.org/10.1021/ic4027392 | Inorg. Chem. 2014, 53, 2122–2132

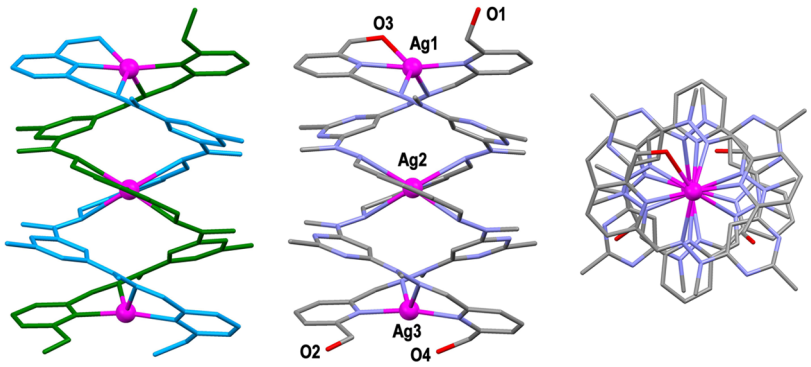

Figure 11. Views of the $[Ag_3(\mathbf{L1})_2]^{3+}$ cation of complex **5** with the individual **L1** ligands color coded (left), the Ag(I) ions and oxygens labeled (middle), and a view down the interior of the helicate (right).

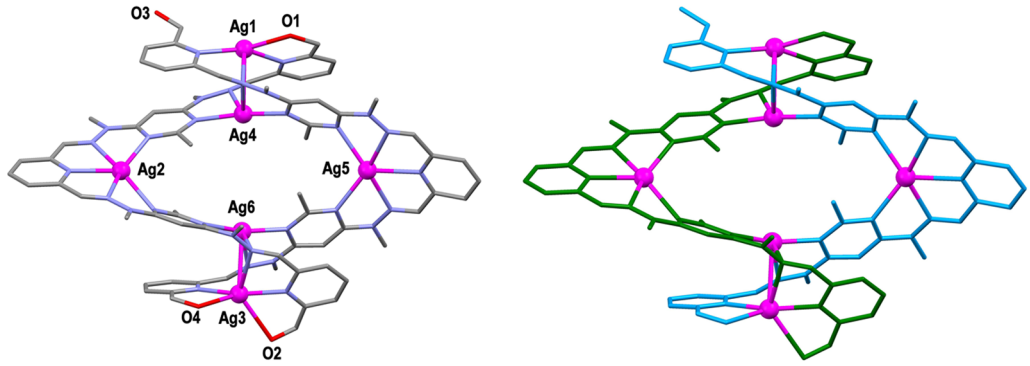

Figure 12. Views of the $[Ag_6(\mathbf{L1})_2]^{6+}$ cation of complex **6** with the Ag(I) ions and oxygens labeled (left) and the individual **L1** ligands color coded (right).

double-helicate $[Ag_3(\mathbf{L1})_2](SO_3CF_3)_3$ (**5**) or the macrocycle-like complex, $[Ag_6(\mathbf{L1})_2](SO_3CF_3)_6$ (**6**), respectively. Despite the radically different structures of complexes **5** and **6**, neither of the X-ray structural solutions appeared to contain any solvent molecules. Electron density due to disordered components was removed from each of the X-ray structural solutions by the use of the PLATON SQUEEZE[21] procedure. However, the number of electrons removed from the asymmetric units of each complex was entirely accounted for by the $SO_3CF_3^-$ anions missing from the solutions.

Complex **5** consisted of two intertwined **L1** strands sharing three Ag(I) ions (Figure 11). At either end of the double helicate were Ag1 and Ag3, both of which were bound to the two terminal py-hyz N donors on each **L1** molecule. Additionally, Ag1 was bound to the hydroxymethyl arm of one of the **L1** molecules, giving it a highly distorted trigonal bipyramidal environment (τ_5 = 0.52).[28] Neither of the hydroxymethyl arms were bound to Ag3; thus, it existed in a highly distorted tetrahedral geometry (τ_4 = 0.54).[29] Ag2 was bound to the three N donors of the central hyz-py-hyz motif on each **L1** molecule, resulting in a relatively rare octahedral geometry.[30] The distances between Ag1 and Ag2, and Ag2 and Ag3 were 5.05 and 5.14 Å, respectively.

In contrast, complex **6** consisted of two **L1** molecules sharing six Ag(I) ions (Figure 12). The Ag(I) ions bound to the terminal py-hyz coordination pockets (Ag1−3 and Ag6) were bound to N donors on both of the **L1** molecules, linking the two ligands together. Ag(I) ions also occupied the central hyz-py-hyz coordination site of each **L1** molecule (Ag2 and Ag5), resulting in the **L1** ligands having horseshoe-like shapes, similar to those seen for complexes **1**−**3**. As a result, complex **6** had a superstructure similar to that of a macrocycle, with a central cavity between Ag2, Ag4, Ag5, and Ag6, and dimensions of 11.2 Å (Ag2−Ag5) and 5.4 Å (Ag4−Ag6).

The Ag(I) ions of complex **6** displayed a range of coordination geometries. Ag1 existed in a distorted square pyramidal geometry (τ_5 = 0.39)[28] with bonds to the terminal py and hyz N donors of each **L1** molecule as well as one of the hydroxymethyl arms and Ag4. The Ag1−Ag4 distance was 2.9670(15) Å. In addition to Ag1, Ag4 was also bound to two hyz-pym N donors on each **L1** molecule, resulting in a five coordination environment which did not resemble either a square pyramid or a trigonal bipyramidal shape (τ_5 = 0.58).[28] The binding environments of Ag3 and Ag6 were analogous to those of Ag1 and Ag4; however, Ag3 was bound to the hydroxymethyl arms of both **L1** molecules and therefore existed in a distorted octahedral environment. Ag2 and Ag5 were both bound to the five N donors of the central pym-hyz-py-hyz-pym section of each **L1** molecule. This resulted in the Ag2 and Ag5 ions adopting unusual perfect square pyramidal geometries (τ_5 values of 0.03 and 0.04, respectively).[28,30]

CONCLUSION

Ligand **L1** was synthesized with hyz-py-hyz and pym-hyz-py coordination sites which underwent contradictory isomerization upon the coordination of Pb(II), Zn(II), and Ag(I) ions. NMR spectroscopy showed that reacting **L1** with either Pb(II), Zn(II), or Ag(I) ions in either CH_3CN or CH_3NO_2 resulted in horseshoe-shaped $M^{n+}{}_3\mathbf{L1}A_{3n}$ complexes. The structures crystallized from these solutions were greatly affected by the metal ion and solvent used. Horseshoe-shaped complexes (**1** and **3**) were crystallized from CH_3CN solutions

dx.doi.org/10.1021/ic4027392 | Inorg. Chem. 2014, 53, 2122−2132

of **L1** with either $Pb(ClO_4)_2·3H_2O$ or $Pb(SO_3CF_3)_2·H_2O$, while a coordination polymer (**2**) was crystallized from a CH_3NO_2 solution of **L1** with $Pb(ClO_4)_2·3H_2O$. Crystals of a zigzag-shaped complex (**4**) were grown from a CH_3CN solution of **L1** with $Zn(SO_3CF_3)_2$, while solutions of $AgSO_3CF_3$ and **L1** in either CH_3CN or CH_3NO_2 resulted in crystals of either a double-helicate complex (**5**) or a macrocycle-like complex (**6**). With the exception of H_2O, none of the solid state structures showed any coordination of solvent molecules to **L1**.

The contradictory fashion of which the hyz-py-hyz and pym-hyz-py coordination sites of **L1** underwent isomerization resulted in a ligand which exhibited significant conformational changes; however, based on the native ligand, and complex shapes from NMR spectroscopy, it appeared that the change in the overall length of the ligand was minimal relative to other pym-hyz molecular strands. It is therefore an appropriate candidate for use in a polymer gel actuator which would act as a negative control for comparison with the planned pym-hyz containing gels. Additionally, the high degree to which the solid state structures of the complexes of **L1** were affected by metal ions and solvents demonstrated that the ligand had a high degree of flexibility and could be used to synthesize interesting crystallographic structures.

■ ASSOCIATED CONTENT

Ⓢ Supporting Information

A discussion of how the disorder of complexes **1**−**6** was treated, pictorial views of complexes **1**−**6** including thermal ellipsoids at the 50% probability level, and selected bond lengths and angles for complexes **1**−**6** in tabulated form; X-ray crystallographic data in CIF form. This material is available free of charge via the Internet at http://pubs.acs.org.

■ AUTHOR INFORMATION

Corresponding Author

*Fax: (+64) 3-479-7906. Phone: (+64) 3-479-7918. E-mail: lhanton@chemistry.otago.ac.nz.

Notes

The authors declare no competing financial interest.

■ ACKNOWLEDGMENTS

We thank the Department of Chemistry, University of Otago, and the New Economic Research Fund of the Foundation for Research, Science and Technology (NERF Grant No UOO-X0808) for financial support.

■ REFERENCES

(1) Stadler, A.-M.; Kyritsakas, N.; Graff, R.; Lehn, J.-M. *Chem.—Eur. J.* **2006**, *12*, 4503−4522.

(2) (a) Schmitt, J.-L.; Stadler, A.-M.; Kyritsakas, N.; Lehn, J.-M. *Helv. Chim. Acta* **2003**, *86*, 1598−1624. (b) Gardinier, K. M.; Khoury, R. G.; Lehn, J.-M. *Chem.—Eur. J.* **2000**, *6*, 4124−4131.

(3) (a) Parizel, N.; Ramírez, J.; Burg, C.; Choua, S.; Bernard, M.; Gambarelli, S.; Maurel, V.; Brelot, L.; Lehn, J.-M.; Turek, P.; Stadler, A.-M. *Chem. Commun.* **2011**, *47*, 10951−10953. (b) Stefankiewicz, A. R.; Harrowfield, J.; Madalan, A.; Rissanen, K.; Sobolev, A. N.; Lehn, J.-M. *Dalton Trans.* **2011**, *40*, 12320−12332. (c) Stefankiewicz, A. R.; Rogez, G.; Harrowfield, J.; Drillon, M.; Lehn, J.-M. *Dalton Trans.* **2009**, 5787−5802. (d) Ramírez, J.; Stadler, A.-M.; Harrowfield, J. M.; Brelot, L.; Huuskonen, J.; Rissanen, K.; Allouche, L.; Lehn, J.-M. *Z. Anorg. Allg. Chem.* **2007**, *633*, 2435−2444. (e) Stadler, A.-M.; Kyritsakas, N.; Vaughan, G.; Lehn, J.-M. *Chem.—Eur. J.* **2007**, *13*, 59−68. (f) Uppadine, L. H.; Lehn, J.-M. *Angew. Chem., Int. Ed. Engl.* **2004**, *43*, 240−243.

(4) Hutchinson, D. J.; Hanton, L. R.; Moratti, S. C. *Inorg. Chem.* **2013**, *52*, 2716−2728.

(5) (a) Yoshida, R. *Adv. Mater.* **2010**, *22*, 3463−3483. (b) Otero, T. F. *J. Mater. Chem.* **2009**, *19*, 681−689. (c) Mirfakhrai, T.; Madden, J. D. W.; Baughman, R. H. *Mater. Today* **2007**, *10*, 30−38. (d) Bassetti, M. J.; Chatterjee, A. N.; Aluru, N. R.; Beebe, D. J. *J. Microelectromech. Syst.* **2005**, *14*, 1198−1207. (e) Baughman, R. H. *Science* **2005**, *308*, 63−65.

(6) (a) Iseda, K.; Kokado, K.; Sada, K. *React. Funct. Polym.* **2013**, *73*, 951−957. (b) Liao, X.; Chen, G.; Jiang, M. *Polym. Chem.* **2013**, *4*, 1733−1745. (c) Takashima, Y.; Hatanka, S.; Otsubo, M.; Nakahata, M.; Kakuta, T.; Hashidzume, A.; Yamaguchi, H.; Harada, A. *Nat. Commun.* **2013**, *3*, 1270−1278. (d) Wei, J.; Yu, Y. *Soft Matter* **2012**, *8*, 8050−8059. (e) Schneider, H.-J.; Strongin, R. M. *Acc. Chem. Res.* **2009**, *42*, 1489−1500. (f) Tanaka, T. *Phys. Rev. Lett.* **1978**, *40*, 820−823.

(7) (a) Hutchinson, D. J.; Cameron, S. A.; Hanton, L. R.; Moratti, S. C. *Inorg. Chem.* **2012**, *51*, 5070−5081. (b) Hutchinson, D. J.; Hanton, L. R.; Moratti, S. C. *Inorg. Chem.* **2011**, *50*, 7637−7649.

(8) Hutchinson, D. J.; Hanton, L. R.; Moratti, S. C. *Inorg. Chem.* **2010**, *49*, 5923−5934.

(9) Hutchinson, D. J.; Hanton, L. R.; Moratti, S. C. Under review.

(10) Kuwabara, J.; Takeuchi, D.; Osakada, K. *Chem. Commun.* **2006**, 3815−3817.

(11) (a) Swift, G. *Acrylic (and methacrylic) Acid Polymers. From Encyclopedia of Polymer Science and Technology*; John Wiley & Sons Inc.: Hoboken, 2004. (b) Coote, M. L.; Davis, T. P. *Copolymerization Kinetics. From Handbook of Radical Polymerization*; John Wiley & Sons Inc.: Hoboken, 2002.

(12) Stadler, A.-M.; Kyritsakas, N.; Lehn, J.-L. *Chem. Commun.* **2004**, 2024−2025.

(13) (a) Alkorta, I.; Elguero, J.; Roussel, C. *Comp. Theor. Chem.* **2011**, *966*, 334−339. (b) Howard, S. T. *J. Am. Chem. Soc.* **1996**, *229*, 10269−10274.

(14) Hutchinson, D. J.; Hanton, L. R.; Moratti, S. C. *Acta. Crystallogr. Sect E.* **2009**, *E65*, o1546.

(15) Shavaleev, N. M.; Scopelliti, R.; Gumy, F.; Büzli, J.-C. G. *Inorg. Chem.* **2009**, *48*, 6178−6191.

(16) (a) Otwinowski, Z.; Minor, W. Processing of X-Ray Diffraction Data Collected in Oscillation Mode; Carter, C. W., Jr., Sweet, R. M., Eds.; In *Methods in Enzymology*, Vol. *276*; Academic Press: New York, 1997; pp 307−326. (b) *SAINT V4, Area Detector Control and Integration Software*; Siemens Analytical X-Ray Systems Inc.: Madison, WI, 1996.

(17) Sheldrick, G. M. *SADABS, Program for Absorption Correction*; University of Göttingen: Göttingen, Germany, 1996.

(18) *Xcalibur/Supernova CCD system, CrysAlisPro Software System*, version 1.171.36.28; Agilent Technologies UK Ltd: Oxford, UK, 2012.

(19) Sheldrick, G. M. *Acta Crystallogr., Sect. A* **1990**, *46*, 467−473.

(20) Altomare, A.; Burla, M. C.; Camalli, M.; Cascarano, G. L.; Giacovazzo, C.; Guagliardi, A.; Moliterni, A. G. G.; Polidori, G.; Spagna, R. *J. Appl. Crystallogr.* **1999**, *32*, 115−119.

(21) Sheldrick, G. M. *SHELXL-97, Program for the Solution of Crystal Structures*; University of Göttingen: Göttingen, Germany, 1997.

(22) Farrugia, L. J. *J. Appl. Crystallogr.* **1999**, *32*, 837−838.

(23) Spek, A. L. *Acta Crystallogr., Sect. A* **1990**, *46*, C34.

(24) (a) Macrae, C. F.; Edgington, P. R.; McCabe, P.; Pidcock, E.; Shields, G. P.; Taylor, R.; Towler, M.; van de Streek, J. *J. Appl. Crystallogr.* **2006**, *39*, 453−457. (b) Bruno, I. J.; Cole, J. C.; Edgington, P. R.; Kessler, M. K.; Macrae, C. F.; McCabe, P.; Pearson, J.; Taylor, R. *Acta Crystallogr., Sect. B* **2002**, *58*, 389−397.

(25) Stadler, A.-M.; Jiang, J.-J.; Wang, H.-P.; Bailly, C. *Chem. Commun.* **2013**, *49*, 3784−3786.

(26) (a) Li, D.; Keresztes, I.; Hopson, R.; Willard, P. G. *Acc. Chem. Res.* **2009**, *42*, 270−280. (b) Giuseppone, N.; Schmitt, J.-L.; Allouche, L.; Lehn, J.-M. *Angew. Chem., Int. Ed.* **2008**, *47*, 2235−2239. (c) Wu, D.; Chen, A.; Johnson, C. S. *J. Am. Chem. Soc.* **1993**, *115*, 4291−4299.

(27) (a) Harrowfield, J. *Helv. Chim. Acta* **2005**, *88*, 2430−2432. (b) Shimoni-Livny, L.; Glusker, J. P.; Bock, C. W. *Inorg. Chem.* **1998**, *37*, 1853−1867.
(28) Addison, A. W.; Rao, T. N.; Reedijk, J.; van Rijn, J.; Verschoor, G. C. *J. Chem. Soc., Dalton Trans.* **1984**, *7*, 1349−1356.
(29) Yang, L.; Powell, D. R.; Houser, R. P. *Dalton Trans.* **2007**, 955−964.
(30) (a) Argyle, V. J.; Woods, L. M.; Roxburgh, M.; Hanton, L. R. *CrystEngComm* **2013**, *15*, 120−134. (b) Young, A. G.; Hanton, L. R. *Coord. Chem. Rev.* **2008**, *252*, 1346−1386.